Journal of Zhejiang University-SCIENCE C (Computers & Electronics)
ISSN 1869-1951 (Print); ISSN 1869-196X (Online)
www.zju.edu.cn/jzus; www.springerlink.com
E-mail: jzus@zju.edu.cn

Trajectory tracking for an autonomous airship using fuzzy adaptive sliding mode control*

Yue-neng YANG, Jie WU, Wei ZHENG†‡

(*College of Aerospace and Materials Engineering, National University of Defense Technology, Changsha 410073, China*)

†E-mail: zhengwei_nudt@163.com

Received Dec. 16, 2011; Revision accepted Mar. 29, 2012; Crosschecked May 31, 2012

Abstract: We present a novel control approach for trajectory tracking of an autonomous airship. First, the dynamics model and the trajectory control problem of an airship are formulated. Second, the sliding mode control law is designed to track a time-varying reference trajectory. To achieve better control performance, fuzzy adaptive sliding mode control is proposed in which the control gains are tuned according to fuzzy rules, and an adaptation law is used to guarantee that the control gains can compensate for model uncertainties of the airship. The stability of the closed-loop control system is proven via the Lyapunov theorem. Finally, simulation results illustrate the effectiveness and robustness of the proposed control scheme.

Key words: Trajectory control, Sliding mode, Fuzzy system, Adaptation law, Uncertainty, External disturbance, Airship
doi:10.1631/jzus.C1100371 **Document code:** A **CLC number:** TP273; V249

1 Introduction

As a typical lighter-than-air (LTA) vehicle, the autonomous airship is a unique and promising platform for many different kinds of applications, such as telecommunication, broadcasting relays, disaster guard, and scientific exploration (Schafer and Reimund, 2002; Chu and Blackmore, 2007; Yang *et al.*, 2012). With the rapid progress of airship technologies, the advanced flight control system plays a key role in the development of the autonomous airship. Nonlinear dynamics, model uncertainties, and external disturbances contribute to the difficulty in maneuvering an airship to track a time-varying reference trajectory. Therefore, trajectory tracking control remains a key technical challenge for the autonomous airship (Yang *et al.*, 2011b).

Several control approaches have been proposed for the trajectory tracking of an airship in the literature. Moutinho and Azinheira (2005) designed the longitudinal and lateral control system of the AURORA airship using the dynamic inversion control method. This control system has limitations because it was developed based on the linear model, neglecting dynamic nonlinearity and coupling effects between longitudinal and lateral motions. Filoktimon and Evangelos (2008) proposed a back-stepping control approach for trajectory tracking of a robotic airship. Lee and Rendon designed a back-stepping design formulation for trajectory control of an unmanned airship (Lee and Lee, 2007; Murguia-Rendon *et al.*, 2009). The design of a back-stepping control system should follow the exact model. However, the airship model always has uncertainties, and the model parameters are difficult to estimate accurately in an operational situation. Zhang *et al.* (2008a) presented an adaptive control solution to the horizontal motion of an airship with neutral buoyancy. In this reference, a novel family of error functions was defined, and the trajectory tracking problem was transformed into an error system stabilization problem.

‡ Corresponding author

* Project supported by the Hunan Provincial Innovation Foundation for Postgraduate (No. CX2011B005) and the National University of Defense Technology Innovation Foundation for Postgraduate (No. B110105), China

Motivated by the results of the aforementioned studies, in this paper we propose a fuzzy adaptive sliding mode control (FASMC) scheme to solve the trajectory tracking problem. Sliding mode control (SMC) provides an effective approach for controlling the systems with nonlinearities, uncertainties, and bounded external disturbances because such control results from a sliding mode on a predefined hyper plane of the state space (Li *et al.*, 2005). However, the undesirable chattering phenomenon is often caused by switching the discontinuous control law from one to another. To attenuate chattering, we introduce fuzzy set theory into SMC to construct the fuzzy sliding mode control (FSMC) for tuning the control gains. In the FSMC system, the control gains continuously vary with the sliding surface according to the fuzzy rules, which effectively attenuates SMC chattering. In addition, an adaptation law is used to guarantee that the gains can compensate for the model uncertainties of the airship (Dong *et al.*, 2009). Moreover, the stability and convergence of the closed-loop control system are proven via the Lyapunov theorem, and effectiveness and robustness of the proposed control scheme are demonstrated via simulation.

2 Modeling and formulation

2.1 Airship kinematics and dynamics

The motion of an airship is usually represented by a set of kinematics and dynamics equations that describe its evolution in a six degrees-of-freedom (6-DOF) space. The coordinate system is depicted in Fig. 1. $O_eX_eY_eZ_e$ is an Earth-fixed inertial frame (E frame), with the origin on the surface of the Earth, the X-axis points north, the Y-axis points east, and the Z-axis points down. $o_bx_by_bz_b$ is the body-fixed frame (B frame), with the origin on the center of the volume, the x-axis points forward, the y-axis points right, and the z-axis points downward (Li *et al.*, 2009). Under the established coordinate frames, the generalized coordinates of an airship are expressed by $\boldsymbol{\eta}=[\boldsymbol{P}, \boldsymbol{\Omega}]^{\mathrm{T}}$, where $\boldsymbol{P}=[x, y, z]^{\mathrm{T}}$ denotes the relative position with respect to the E frame, and $\boldsymbol{\Omega}=[\theta, \psi, \varphi]^{\mathrm{T}}$ defines the attitude angles, including the pitch, yaw, and roll angles. The generalized velocities of an airship are expressed by $\boldsymbol{V}=[\boldsymbol{v}, \boldsymbol{\omega}]^{\mathrm{T}}$, where $\boldsymbol{v}=[u, v, w]^{\mathrm{T}}$ defines the linear velocities in the B frame, namely, the forward, lateral, and vertical velocities, and $\boldsymbol{\omega}=[p, q, r]^{\mathrm{T}}$ denotes the angular velocities about each axis of the B frame (Yang *et al.*, 2011a; 2011c).

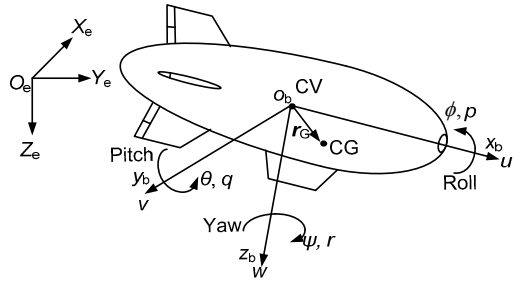

Fig. 1 Coordinate systems of an airship
CV: center of the volume; CG: center of the gravity

Considering these motion variables, the 6-DOF kinematics equations of an airship can be written as (Yang *et al.*, 2011b; 2011c)

$$\dot{\boldsymbol{\eta}} = \boldsymbol{J}(\boldsymbol{\eta})\boldsymbol{V}, \tag{1}$$

where

$$\boldsymbol{J}(\boldsymbol{\eta}) = \begin{bmatrix} \boldsymbol{J}_1 & \boldsymbol{0}_{3\times3} \\ \boldsymbol{0}_{3\times3} & \boldsymbol{J}_2 \end{bmatrix}, \tag{2}$$

with $\boldsymbol{J}_1$ and $\boldsymbol{J}_2$ being the rotation matrix from the B frame to the E frame and the transform matrix from angular velocities to attitude angle rates, respectively. The corresponding expressions of the two matrices can be expressed as follows:

$$\boldsymbol{J}_1 = \begin{bmatrix} \cos\psi\cos\theta & \cos\psi\sin\theta\sin\phi & \cos\psi\sin\theta\cos\phi \\ & & +\sin\psi\sin\phi \\ \sin\psi\cos\theta & \sin\psi\sin\theta\sin\phi & \sin\psi\sin\theta\cos\phi \\ & +\cos\psi\cos\phi & -\cos\psi\sin\phi \\ -\sin\theta & \cos\theta\sin\phi & \cos\theta\cos\phi \end{bmatrix},$$

$$\boldsymbol{J}_2 = \begin{bmatrix} 0 & \cos\phi & -\sin\phi \\ 0 & \sec\theta\sin\phi & \sec\theta\cos\phi \\ 1 & \tan\theta\sin\phi & \tan\theta\cos\phi \end{bmatrix}.$$

The 6-DOF dynamics equations of an airship can be derived as follows (Cai *et al.*, 2007; Lee and Lee, 2007):

$$\boldsymbol{M}\dot{\boldsymbol{V}} + \boldsymbol{C}(\boldsymbol{V})\boldsymbol{V} + \boldsymbol{D}(\boldsymbol{V})\boldsymbol{V} + \boldsymbol{G}(\boldsymbol{\eta}) = \boldsymbol{\tau}, \tag{3}$$

where $\boldsymbol{M}$ is the inertia matrix, $\boldsymbol{C}(\boldsymbol{V})$ is the centrifugal and Coriolis matrix, $\boldsymbol{D}(\boldsymbol{V})$ is the damping matrix, $\boldsymbol{G}(\boldsymbol{\eta})$ is the vector of gravitational and buoyant forces and

moments, and $\boldsymbol{\tau}$ denotes the control forces and moments (Cai *et al.*, 2007).

2.2 Trajectory motion model

The trajectory tracking problem for an airship is the design of a control law that asymptotically stabilizes both the position and the orientation. Therefore, we can restrict the six-dimensional dynamics to the horizontal plane by making the following assumptions:

Assumption 1 The dynamics associated with the pitch and roll motions are negligible (Zhang, 2009). When the airship is cruising at a constant altitude (Fig. 2), pitch and roll variables are very small, and therefore their effect on the motion in the horizontal plane can be neglected.

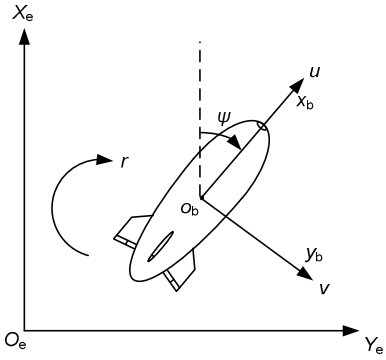

Fig. 2 Airship motion in the horizontal plane

Assumption 2 We consider an airship with neutral buoyancy; that is, the gravitation is equal to buoyancy. Therefore, the resultant forces of gravitation and buoyancy have no effect on the dynamics in the horizontal motion of an airship (Zhang *et al.*, 2008b).

Under these assumptions, a simplified 3-DOF model of planar motion is obtained as follows:

$$\boldsymbol{M}\dot{\boldsymbol{V}}+\boldsymbol{C}(\boldsymbol{V})\boldsymbol{V}+\boldsymbol{D}(\boldsymbol{V})\boldsymbol{V}=\boldsymbol{\tau}, \tag{4}$$

$$\dot{\boldsymbol{\eta}}=\boldsymbol{J}(\boldsymbol{\eta})\boldsymbol{V}, \tag{5}$$

where

$$\boldsymbol{M}=\begin{bmatrix} m-X_{\dot{u}} & 0 & 0 \\ 0 & m-Y_{\dot{v}} & 0 \\ 0 & 0 & I_{33}-N_{\dot{r}} \end{bmatrix},$$

$$\boldsymbol{C}(\boldsymbol{V})=\begin{bmatrix} 0 & 0 & -(m-Y_{\dot{v}})v \\ 0 & 0 & (m-X_{\dot{u}})u \\ (m-Y_{\dot{v}})v & -(m-X_{\dot{u}})u & 0 \end{bmatrix},$$

$$\boldsymbol{D}(\boldsymbol{V})=\begin{bmatrix} -X_u & 0 & 0 \\ 0 & -Y_v & 0 \\ 0 & 0 & -N_r \end{bmatrix},$$

$$\boldsymbol{J}(\boldsymbol{\Omega})=\begin{bmatrix} \cos\psi & -\sin\psi & 0 \\ \sin\psi & \cos\psi & 0 \\ 0 & 0 & 1 \end{bmatrix},$$

where m is the gross mass, $X_{\dot{u}}$, $Y_{\dot{v}}$, $N_{\dot{r}}$, X_u, Y_v, and N_r are the added inertial parameters (Cai, 2006), $\boldsymbol{\eta}=[x, y, \psi]^{\mathrm{T}}$ denotes the position and orientation in the E frame, $\boldsymbol{V}=[u, v, r]^{\mathrm{T}}$ denotes the forward, lateral, and yaw angular velocities, $\boldsymbol{\tau}=[\tau_u, \tau_v, \tau_r]^{\mathrm{T}}$ denotes the forward force, lateral force, and yaw moment, and I_{33} denotes the moment of inertia about the o_bz_b axis.

Eq. (4) is evidently only an explicit function of $\boldsymbol{V}$, but the problem formulation should be an explicit function of $\boldsymbol{\eta}$. Therefore, we should transform Eq. (4) into an explicit function of $\boldsymbol{\eta}$ (Bagheri and Moghaddam, 2009).

From Eq. (5), we obtain

$$\boldsymbol{V}=\boldsymbol{J}^{-1}(\boldsymbol{\eta})\dot{\boldsymbol{\eta}}. \tag{6}$$

Differentiating Eq. (6), we derive

$$\begin{aligned}\dot{\boldsymbol{V}}&=\frac{\partial\boldsymbol{J}^{-1}(\boldsymbol{\eta})}{\partial t}\dot{\boldsymbol{\eta}}+\boldsymbol{J}^{-1}(\boldsymbol{\eta})\ddot{\boldsymbol{\eta}}\\&=-\boldsymbol{J}^{-1}(\boldsymbol{\eta})\dot{\boldsymbol{J}}(\boldsymbol{\eta})\boldsymbol{J}^{-1}(\boldsymbol{\eta})\dot{\boldsymbol{\eta}}+\boldsymbol{J}^{-1}(\boldsymbol{\eta})\ddot{\boldsymbol{\eta}}.\end{aligned} \tag{7}$$

Substituting Eq. (7) into Eq. (4), we obtain

$$\begin{aligned}&\boldsymbol{M}\boldsymbol{J}^{-1}(\boldsymbol{\eta})\ddot{\boldsymbol{\eta}}-\boldsymbol{M}\boldsymbol{J}^{-1}(\boldsymbol{\eta})\dot{\boldsymbol{J}}(\boldsymbol{\eta})\boldsymbol{J}^{-1}(\boldsymbol{\eta})\dot{\boldsymbol{\eta}}\\&+\boldsymbol{C}(\boldsymbol{V})\boldsymbol{J}^{-1}(\boldsymbol{\eta})\dot{\boldsymbol{\eta}}+\boldsymbol{D}(\boldsymbol{V})\boldsymbol{J}^{-1}(\boldsymbol{\eta})\dot{\boldsymbol{\eta}}\\&=\boldsymbol{M}\boldsymbol{J}^{-1}(\boldsymbol{\eta})\ddot{\boldsymbol{\eta}}+[\boldsymbol{C}(\boldsymbol{V})-\boldsymbol{M}\boldsymbol{J}^{-1}(\boldsymbol{\eta})\dot{\boldsymbol{J}}(\boldsymbol{\eta})]\\&\cdot\boldsymbol{J}^{-1}(\boldsymbol{\eta})\dot{\boldsymbol{\eta}}+\boldsymbol{D}(\boldsymbol{V})\boldsymbol{J}^{-1}(\boldsymbol{\eta})\dot{\boldsymbol{\eta}}\\&=\boldsymbol{\tau}.\end{aligned} \tag{8}$$

Define

$$\boldsymbol{M}_{\eta}=\boldsymbol{M}\boldsymbol{J}^{-1}(\boldsymbol{\eta}), \tag{9}$$

$$\boldsymbol{C}_{\eta}(\boldsymbol{V})=[\boldsymbol{C}(\boldsymbol{V})-\boldsymbol{M}\boldsymbol{J}^{-1}(\boldsymbol{\eta})\dot{\boldsymbol{J}}(\boldsymbol{\eta})]\boldsymbol{J}^{-1}(\boldsymbol{\eta}), \tag{10}$$

$$\boldsymbol{D}_{\eta}(\boldsymbol{V})=\boldsymbol{D}(\boldsymbol{V})\boldsymbol{J}^{-1}(\boldsymbol{\eta}). \tag{11}$$

Eq. (4) can then be rewritten as

$$\boldsymbol{M}_\eta(\boldsymbol{\eta})\ddot{\boldsymbol{\eta}} + \boldsymbol{C}_\eta(\boldsymbol{\eta})\dot{\boldsymbol{\eta}} + \boldsymbol{D}_\eta(\boldsymbol{\eta})\dot{\boldsymbol{\eta}} = \boldsymbol{\tau}. \quad (12)$$

Considering model uncertainties, Eq. (12) can be expressed as follows:

$$\hat{\boldsymbol{M}}_\eta\ddot{\boldsymbol{\eta}} + \hat{\boldsymbol{C}}_\eta\dot{\boldsymbol{\eta}} + \hat{\boldsymbol{D}}_\eta\dot{\boldsymbol{\eta}} = \boldsymbol{\tau}, \quad (13)$$

where $\hat{\boldsymbol{M}}_\eta = \boldsymbol{M}_\eta + \Delta\boldsymbol{M}_\eta$, $\hat{\boldsymbol{C}}_\eta = \boldsymbol{C}_\eta + \Delta\boldsymbol{C}_\eta$, and $\hat{\boldsymbol{D}}_\eta = \boldsymbol{D}_\eta + \Delta\boldsymbol{D}_\eta$, $\Delta\boldsymbol{M}_\eta$, $\Delta\boldsymbol{C}_\eta$, and $\Delta\boldsymbol{D}_\eta$ are the uncertainties of the inertia matrix, centrifugal and Coriolis matrix, and damping matrix, respectively.

We then define

$$\Delta\boldsymbol{f} = \Delta\boldsymbol{M}_\eta\ddot{\boldsymbol{\eta}} + \Delta\boldsymbol{C}_\eta\dot{\boldsymbol{\eta}} + \Delta\boldsymbol{D}_\eta\dot{\boldsymbol{\eta}} \quad (14)$$

such that Eq. (13) can be rewritten as (Bagheri and Moghaddam, 2009)

$$\boldsymbol{M}_\eta(\boldsymbol{\eta})\ddot{\boldsymbol{\eta}} + \boldsymbol{C}_\eta(\boldsymbol{\eta})\dot{\boldsymbol{\eta}} + \boldsymbol{D}_\eta(\boldsymbol{\eta})\dot{\boldsymbol{\eta}} + \Delta\boldsymbol{f} = \boldsymbol{\tau}. \quad (15)$$

3 Control design

3.1 Control strategy

The control objective is to design a control law that causes the airship to track a desired trajectory asymptotically. The control inputs should be designed to drive the airship to follow the desired trajectory $\boldsymbol{\eta}_\mathrm{d}=[x_\mathrm{d}, y_\mathrm{d}, \psi_\mathrm{d}]^\mathrm{T}$, as given by

$$x_\mathrm{d} = x_\mathrm{d}(t), \quad y_\mathrm{d} = y_\mathrm{d}(t), \quad \psi_\mathrm{d} = \psi_\mathrm{d}(t), \quad (16)$$

where $x_\mathrm{d}(t)$ and $y_\mathrm{d}(t)$ are the desired time-varying positions, and $\psi_\mathrm{d}(t)$ is the desired time-varying orientation, such that

$$\lim_{t\to\infty}\|\boldsymbol{\eta} - \boldsymbol{\eta}_\mathrm{d}\| = 0. \quad (17)$$

In this section we propose an FASMC scheme for the trajectory tracking problem. First, the SMC law is designed to track the desired trajectory. Second, the fuzzy system is introduced for tuning the control gains, and the adaptation law is used to estimate the model uncertainties (Liu, 2008). Fig. 3 depicts the block diagram of the control system.

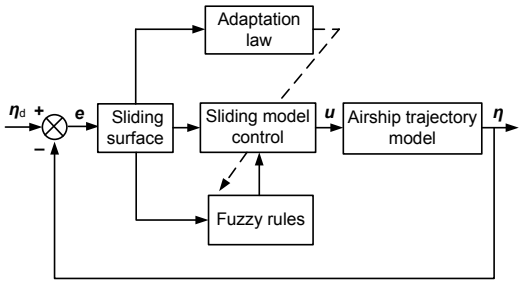

Fig. 3 The system block diagram of the fuzzy adaptive sliding mode control (FASMC) scheme

3.2 Sliding mode control

In this subsection, we use the SMC method to design the trajectory tracking controller. In general, SMC design is divided into two steps. The first step is defining the sliding surface, and the second step is designing the control law, such that the system states approach and remain on the intersection of the sliding surface (Li *et al.*, 2005).

The tracking error is defined as

$$\boldsymbol{e} = \boldsymbol{\eta} - \boldsymbol{\eta}_\mathrm{d}. \quad (18)$$

The sliding surface is selected as

$$\boldsymbol{s} = \dot{\boldsymbol{e}} + \boldsymbol{c}\boldsymbol{e}, \quad (19)$$

where $\boldsymbol{c}$=diag$\{c_1, c_2, c_3\}$, and $c_i>0$ (i=1, 2, 3).

We define

$$\dot{\boldsymbol{\eta}}_\mathrm{r} = \dot{\boldsymbol{\eta}} - \boldsymbol{s} = \dot{\boldsymbol{\eta}}_\mathrm{d} - \boldsymbol{c}\boldsymbol{e} \quad (20)$$

such that Eq. (19) can be rewritten as

$$\boldsymbol{s} = \dot{\boldsymbol{\eta}} - \dot{\boldsymbol{\eta}}_\mathrm{r}. \quad (21)$$

We adopt the following reaching law (Bagheri and Moghaddam, 2009):

$$\dot{\boldsymbol{s}} = -\boldsymbol{\rho}\boldsymbol{s} - \boldsymbol{k}\,\mathrm{sign}(\boldsymbol{s}), \quad (22)$$

where $\boldsymbol{\rho}$ and $\boldsymbol{k}$ are both diagonal positive definite matrices, with $\boldsymbol{\rho}$=diag$\{\rho_1, \rho_2, \rho_3\}$, $\rho_i>0$ (i=1, 2, 3) and $\boldsymbol{k}$=diag$\{k_1, k_2, k_3\}$, $k_i>0$ (i=1, 2, 3).

By adopting the abovementioned sliding surface and reaching law, we design the SMC law as follows:

$$\begin{aligned}\boldsymbol{\tau} = {} & \boldsymbol{M}_\eta(\boldsymbol{\eta})\ddot{\boldsymbol{\eta}}_\mathrm{r} + \boldsymbol{C}_\eta(\boldsymbol{\eta})\dot{\boldsymbol{\eta}}_\mathrm{r} + \boldsymbol{D}_\eta(\boldsymbol{\eta})\dot{\boldsymbol{\eta}}_\mathrm{r} \\ & + \Delta\boldsymbol{f} - \boldsymbol{\rho}\boldsymbol{s} - \boldsymbol{k}\,\mathrm{sign}(\boldsymbol{s}).\end{aligned} \quad (23)$$

The stability of the control system will be analyzed using the Lyapunov theorem.

Theorem 1 We consider the system defined by Eq. (15) and the sliding mode defined as Eq. (19). Global asymptotic stability is guaranteed by designing the control law as Eq. (23).

Proof The Lyapunov function is selected as

$$V=\frac{1}{2}\boldsymbol{s}^{\mathrm{T}}\boldsymbol{M}\boldsymbol{s}. \tag{24}$$

Since V is positive definite and unbounded, global asymptotic stability can be ensured if

$$\dot{V}<0. \tag{25}$$

Differentiating Eq. (24), we obtain

$$\dot{V}=\frac{1}{2}(\dot{\boldsymbol{s}}^{\mathrm{T}}\boldsymbol{M}\boldsymbol{s}+\boldsymbol{s}^{\mathrm{T}}\dot{\boldsymbol{M}}\boldsymbol{s}+\boldsymbol{s}^{\mathrm{T}}\boldsymbol{M}\dot{\boldsymbol{s}}). \tag{26}$$

Substituting Eqs. (15) and (22) into Eq. (26), we derive

$$\dot{V}=\boldsymbol{s}^{\mathrm{T}}(-\boldsymbol{\rho}\boldsymbol{s}+\Delta\boldsymbol{f}-\boldsymbol{k})=-\boldsymbol{s}^{\mathrm{T}}\boldsymbol{\rho}\boldsymbol{s}+\boldsymbol{s}^{\mathrm{T}}(\Delta\boldsymbol{f}-\boldsymbol{k}). \tag{27}$$

From Eq. (26), we know that $\dot{V}<0$ can be ensured if $\Delta\boldsymbol{f}\leqslant\boldsymbol{k}$. This condition guarantees that the sliding mode can be reached in finite time. Therefore, the asymptotic stability of the control system has been analyzed and verified.

3.3 Fuzzy adaptive control

3.3.1 Fuzzy system

The reaching law given by Eq. (22) is used to design the SMC law in the above subsection. If $\boldsymbol{s}\to\boldsymbol{0}$, then $\boldsymbol{\rho}\boldsymbol{s}\to\boldsymbol{0}$, whereas the term $\boldsymbol{k}$sign($\boldsymbol{s}$) does not reach zero. The system state generates chattering because of the repeated switching of the sliding surface. The intensity of the chattering is determined by the gain $\boldsymbol{k}$. To accelerate the reaching and reduce chattering, a fuzzy system is introduced to solve this problem. We selected $\boldsymbol{s}$ as the fuzzy control input, and let $\boldsymbol{k}$ be the fuzzy control output. Therefore, the gain $\boldsymbol{k}$ can be tuned according to the change of $\boldsymbol{s}$ via the fuzzy rules (Li *et al.*, 2008).

The fuzzy sets of input and output variables are both defined as {NB, NS, ZO, PS, PB}, where NB is negative big, NS is negative small, ZO is zero, PS is positive small, and PB is positive big.

Supposing the fuzzy system in this study is constructed from the following IF-THEN rules (Liu *et al.*, 2010):

$$R^{(j)}\text{: IF } s_i \text{ is } F_s^j \text{ THEN } k_i \text{ is } B^j,$$

where $s_i\in\boldsymbol{s}$, $k_i\in\boldsymbol{k}$, the set of s_i is composed of F_s^j, and B^j is the output of the jth fuzzy rule.

We construct the fuzzy basic function as (Fateh, 2010)

$$\xi_i(x)=\prod_{j=1}^{n}\mu_{F_j^i}(x_j)\Big/\sum_{i=1}^{m}\prod_{j=1}^{n}\mu_{F_j^i}(x_j), \tag{28}$$

where x_j is a discretional variable, $\mu_{F_j^i}(x_j)$ is the membership function of x_j, and m and n denote the numbers of fuzzy rules.

We then select the following Gaussian membership functions (Liu, 2008):

$$\begin{aligned}
&\mu_{\mathrm{NB}}(x_j)=\exp\{-[(x_j+\pi/6)/(\pi/24)]^2\},\\
&\mu_{\mathrm{NS}}(x_j)=\exp\{-[(x_j+\pi/12)/(\pi/24)]^2\},\\
&\mu_{\mathrm{ZO}}(x_j)=\exp\{-[x_j/(\pi/24)]^2\},\\
&\mu_{\mathrm{PS}}(x_j)=\exp\{-[(x_j-\pi/12)/(\pi/24)]^2\},\\
&\mu_{\mathrm{PB}}(x_j)=\exp\{-[(x_j-\pi/6)/(\pi/24)]^2\},
\end{aligned}$$

The corresponding membership functions of these fuzzy sets labels are depicted in Fig. 4.

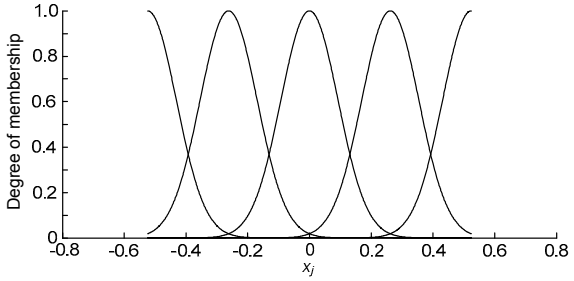

Fig. 4 The membership functions for x_j

Based on the aforementioned fuzzy sets and membership functions, the fuzzy rules are described in Table 1.

Table 1 Fuzzy control rules

s_i	NB	NS	ZO	PS	PB
k_i	NB	NS	ZO	PS	PB

NB: negative big; NS: negative small; ZO: zero; PS: positive small; PB: positive big

Specifically, using the product inference engine, singleton fuzzifier, and center average defuzzifier (Fateh, 2010), we derive

$$k_i=\frac{\sum_{i=1}^{m}\left(\gamma_{k_i}^{i}\prod_{j=1}^{n}\mu_{F_j^i}(s_j)\right)}{\sum_{i=1}^{m}\prod_{j=1}^{n}\mu_{F_j^i}(s_j)}=\boldsymbol{\Gamma}_{k_i}^{\mathrm{T}}\boldsymbol{\xi}_{k_i}(s_i),\tag{29}$$

where $\boldsymbol{\xi}_{k_i}(s_i)=[\xi_{k_i}^1(s_i),\xi_{k_i}^2(s_i),\cdots,\xi_{k_i}^m(s_i)]^{\mathrm{T}}$ is the height vector of the membership functions of k_i, and $\boldsymbol{\Gamma}_{k_i}^{\mathrm{T}}=[\gamma_{k_i}^1,\gamma_{k_i}^2,\cdots,\gamma_{k_i}^m]^{\mathrm{T}}$ is the center vector of the membership functions of k_i.

The control gain k_i can then be tuned using the proposed fuzzy system.

3.3.2 Adaptation law

Considering the model uncertainties in Eq. (14), we employ an adaptation law to estimate the uncertainties of the control system (Liu, 2008).

Considering Eq. (27), we select the following formula to approximate the model uncertainties (Yang *et al.*, 2000; Tong and Li, 2003):

$$\boldsymbol{k}=\boldsymbol{\Gamma}^{\mathrm{T}}\boldsymbol{\xi}(\boldsymbol{s}),\tag{30}$$

where

$$\boldsymbol{\xi}(\boldsymbol{s})=[\xi_{k_1},\xi_{k_2},\cdots,\xi_{k_m}]^{\mathrm{T}},$$
$$\boldsymbol{\Gamma}=[\Gamma_{k_1},\Gamma_{k_2},\cdots,\Gamma_{k_m}]^{\mathrm{T}}.$$

According to the universal approximation theorem (Li *et al.*, 2008), the following inequality is always satisfied:

$$\left\|\Delta\boldsymbol{f}-\hat{\boldsymbol{\Gamma}}^{\mathrm{T}}\boldsymbol{\xi}(\boldsymbol{s})\right\|\le\varepsilon,\tag{31}$$

where $\hat{\boldsymbol{\Gamma}}$ is the estimation of $\boldsymbol{\Gamma}$, and ε is a positive number.

The error $\boldsymbol{\Gamma}_{\mathrm{e}}$ can be given as follows:

$$\boldsymbol{\Gamma}_{\mathrm{e}}=\boldsymbol{\Gamma}-\hat{\boldsymbol{\Gamma}}.\tag{32}$$

Let the adaptation law be (Neila and Damak, 2011)

$$\dot{\boldsymbol{\Gamma}}_{\mathrm{e}}=\boldsymbol{s}^{\mathrm{T}}\boldsymbol{\xi}(\boldsymbol{s}).\tag{33}$$

The following Lyapunov function is then selected (Liu, 2008):

$$V=\frac{1}{2}\boldsymbol{s}^{\mathrm{T}}\boldsymbol{M}\boldsymbol{s}+\frac{1}{2}\boldsymbol{\Gamma}_{\mathrm{e}}^{\mathrm{T}}\boldsymbol{\Gamma}_{\mathrm{e}}.\tag{34}$$

Differentiating Eq. (34), we obtain

$$\dot{V}=\frac{1}{2}(\dot{\boldsymbol{s}}^{\mathrm{T}}\boldsymbol{M}\boldsymbol{s}+\boldsymbol{s}^{\mathrm{T}}\dot{\boldsymbol{M}}\boldsymbol{s}+\boldsymbol{s}^{\mathrm{T}}\boldsymbol{M}\dot{\boldsymbol{s}})+\frac{1}{2}(\dot{\boldsymbol{\Gamma}}_{\mathrm{e}}^{\mathrm{T}}\boldsymbol{\Gamma}_{\mathrm{e}}+\boldsymbol{\Gamma}_{\mathrm{e}}^{\mathrm{T}}\dot{\boldsymbol{\Gamma}}_{\mathrm{e}}).\tag{35}$$

Substituting Eqs. (15) and (22) into Eq. (35), we derive

$$\begin{aligned}\dot{V}&=\boldsymbol{s}^{\mathrm{T}}(-\boldsymbol{\rho}\boldsymbol{s}+\Delta\boldsymbol{f}-\boldsymbol{k})+\boldsymbol{\Gamma}_{\mathrm{e}}^{\mathrm{T}}\dot{\boldsymbol{\Gamma}}_{\mathrm{e}}\\&=-\boldsymbol{s}^{\mathrm{T}}\boldsymbol{\rho}\boldsymbol{s}+\boldsymbol{s}^{\mathrm{T}}(\Delta\boldsymbol{f}-\boldsymbol{k})+\boldsymbol{\Gamma}_{\mathrm{e}}^{\mathrm{T}}\dot{\boldsymbol{\Gamma}}_{\mathrm{e}}.\end{aligned}\tag{36}$$

Substituting Eqs. (30) and (32) into Eq. (36) yields

$$\begin{aligned}\dot{V}&=-\boldsymbol{s}^{\mathrm{T}}\boldsymbol{\rho}\boldsymbol{s}+\boldsymbol{s}^{\mathrm{T}}\{\Delta\boldsymbol{f}-[\boldsymbol{\Gamma}_{\mathrm{e}}^{\mathrm{T}}\boldsymbol{\xi}(\boldsymbol{s})+\hat{\boldsymbol{\Gamma}}^{\mathrm{T}}\boldsymbol{\xi}(\boldsymbol{s})]\}+\boldsymbol{\Gamma}_{\mathrm{e}}^{\mathrm{T}}\dot{\boldsymbol{\Gamma}}_{\mathrm{e}}\\&=-\boldsymbol{s}^{\mathrm{T}}\boldsymbol{\rho}\boldsymbol{s}+\boldsymbol{s}^{\mathrm{T}}[\Delta\boldsymbol{f}-\hat{\boldsymbol{\Gamma}}^{\mathrm{T}}\boldsymbol{\xi}(\boldsymbol{s})]+\boldsymbol{\Gamma}_{\mathrm{e}}^{\mathrm{T}}[-\boldsymbol{s}^{\mathrm{T}}\boldsymbol{\xi}(\boldsymbol{s})+\dot{\boldsymbol{\Gamma}}_{\mathrm{e}}].\end{aligned}\tag{37}$$

Substituting the adaptation law (33) into Eq. (37), we derive

$$\dot{V}=-\boldsymbol{s}^{\mathrm{T}}\boldsymbol{\rho}\boldsymbol{s}+\boldsymbol{s}^{\mathrm{T}}[\Delta\boldsymbol{f}-\hat{\boldsymbol{\Gamma}}^{\mathrm{T}}\boldsymbol{\xi}(\boldsymbol{s})].\tag{38}$$

From Eq. (31), we obtain (Sun *et al.*, 1999)

$$\left\|\Delta\boldsymbol{f}-\hat{\boldsymbol{\Gamma}}^{\mathrm{T}}\boldsymbol{\xi}(\boldsymbol{s})\right\|\le\varepsilon\le\lambda_i\|\boldsymbol{s}\|,\tag{39}$$

where $0<\lambda_i<1$ (i=1, 2, 3).

Considering Eq. (39), Eq. (38) can be expressed as

$$\dot{V}\le-\boldsymbol{s}^{\mathrm{T}}\boldsymbol{\rho}\boldsymbol{s}+\boldsymbol{s}^{\mathrm{T}}\boldsymbol{\lambda}\boldsymbol{s}=\boldsymbol{s}^{\mathrm{T}}(\boldsymbol{\lambda}-\boldsymbol{\rho})\boldsymbol{s}=\sum_{i=1}^{3}(\lambda_i-\rho_i)s_i^2,\tag{40}$$

where $\boldsymbol{\lambda}$=diag$\{\lambda_1, \lambda_2, \lambda_3\}$.

$\dot{V}<0$ can be ensured if $\rho_i>\lambda_i$; that is,

$$\dot{V}\le\sum_{i=1}^{3}(\lambda_i-\rho_i)s_i^2<0,\quad\rho_i>\lambda_i.\tag{41}$$

As shown by Eq. (40), if $\boldsymbol{s}$=$\boldsymbol{0}$, then $\dot{V}=0$. Thus, we have

$$\lim_{t\to\infty}\boldsymbol{s}=\lim_{t\to\infty}(\dot{\boldsymbol{e}}+\boldsymbol{c}\boldsymbol{e})=\lim_{t\to\infty}[(\dot{\boldsymbol{\eta}}-\dot{\boldsymbol{\eta}}_{\mathrm{d}})+\boldsymbol{c}(\boldsymbol{\eta}-\boldsymbol{\eta}_{\mathrm{d}})]=\boldsymbol{0}.\tag{42}$$

Considering that $\boldsymbol{c}$ is a positive definite matrix, we

obtain the following equations according to Eq. (42):

$$\lim_{t\to\infty}\boldsymbol{\eta}=\boldsymbol{\eta}_{\mathrm{d}},\ \text{and}\ \lim_{t\to\infty}\dot{\boldsymbol{\eta}}=\dot{\boldsymbol{\eta}}_{\mathrm{d}}. \tag{43}$$

The proposed control scheme has proven capable of driving the airship to asymptotically track a designed trajectory via Eq. (43). Thus, the proposed control scheme is feasible for trajectory tracking control of an airship.

4 Simulation study

This section illustrates the performance of the designed trajectory tracking control system via numerical simulation. The control system was simulated using the variable step Runge-Kutta integrator in MATLAB. The model parameters of the airship (Cai, 2006) are given in Table 2.

Table 2 Model parameters of the airship

Parameter	Value	Parameter	Value
m (kg)	239	$X_{\dot{u}}$ (kg)	−4.235
I_x (kg·m^2)	833.2	$Y_{\dot{v}}$ (kg)	−21.668
I_y (kg·m^2)	13 229.5	$N_{\dot{r}}$ (kg·m^2)	−3.423
I_z (kg·m^2)	12 826.7	X_u (kg)	216.7
I_{xz} (kg·m^2)	1047.6	Y_v (kg)	215
z_{G} (m)	0.902	N_r (kg·m^2)	50.2

Considering that the turning circle maneuver is an important practical trajectory maneuver that the airship needs to perform frequently, we examine the control performance of circle trajectory tracking using the designed control scheme. The desired trajectory is generated using the following command generator:

$$\begin{cases}\dot{x}_{\mathrm{d}}=5\cos(0.01t),\\ \dot{y}_{\mathrm{d}}=5\sin(0.01t),\\ \dot{\psi}_{\mathrm{d}}=0.01.\end{cases} \tag{44}$$

The desired velocities were selected as $\boldsymbol{v}_{\mathrm{d}}=[u_{\mathrm{d}},\ v_{\mathrm{d}},\ r_{\mathrm{d}}]^{\mathrm{T}}=[5\ \text{m/s},\ 0\ \text{m/s},\ 0.01\ \text{rad/s}]^{\mathrm{T}}$, and the initial state of the airship was set to be $\boldsymbol{\eta}_0=[x_0, y_0, \psi_0]^{\mathrm{T}}=[500\ \text{m},\ 500\ \text{m},\ -\pi/2]^{\mathrm{T}}$. Simulation results were obtained for two cases: (1) the model parameters are known and (2) there are parameter uncertainties and external disturbances. In all of the following simulations we used the same controller structure for trajectory tracking control. Specifically, we selected the control gains ρ_1=0.01, ρ_2=0.02, and ρ_3=0.05.

Case 1: The following simulations concern the trajectory tracking control design based on the accurate model parameters. Simulation results of this case are shown in Figs. 5 and 6.

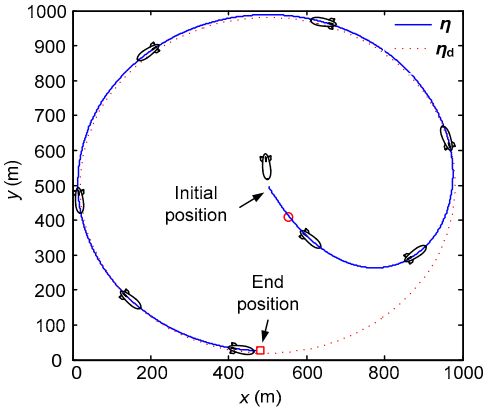

Fig. 5 Circle trajectory tracking with accurate parameters and without disturbances

Fig. 5 displays the simulation results of circle trajectory tracking control with accurate parameters and without external disturbances. The dotted line depicts the desired trajectory whereas the solid line depicts the actual trajectory. It is clear that the airship traces a perfect circle trajectory.

Fig. 6a displays the tracking errors of position and orientation, which are gradually convergent to zero. These simulation results demonstrate that the trajectory tracking is accomplished with precision using the designed controller.

Fig. 6b displays the airship velocities, namely, the forward speed, lateral speed, and yaw angular velocity. As shown in Fig. 6b, the forward speed converges to 5 m/s within 200 s, the lateral speed converges to 0 m/s within 100 s, and the yaw angular velocity rapidly converges to 0.01 rad/s. The actual velocities of the airship can also be controlled to track the velocity of the desired trajectory with high precision.

The evolution of control gains is shown in Fig. 6c. The control gain k_i is tuned via the fuzzy rules and the adaptation law. The control gain converges to a certain constant value after trajectory tracking is accomplished.

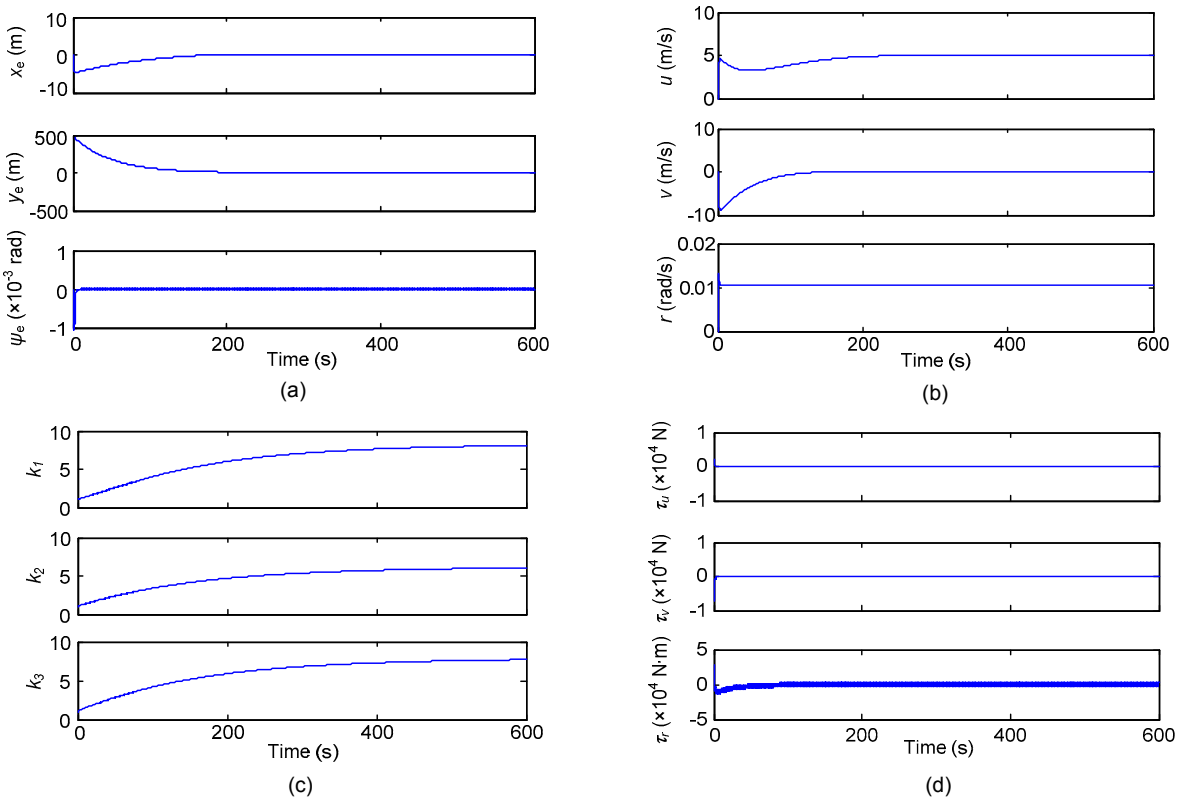

Fig. 6 Tracking errors (a), generalized velocities (b), control gains (c), and control inputs (d) with accurate parameters and without disturbances

The control inputs are shown in Fig. 6d. As shown by the transition curves of the control inputs in Fig. 6d, the changes in τ_u, τ_v, and τ_r are gradual and perfectly meet the controlling force and moment requirements for trajectory tracking control.

Case 2: We concern the robustness properties of the designed control scheme to parameter uncertainties and external disturbances. We conducted simulations in which errors of the order of 5% on all parameters in Table 2 were assumed. In practice, the external disturbances mainly may be the wind disturbances. We assume that the wind disturbances in the lateral direction are d_w=10cos$t$ m/s, where 10 m/s is the wind velocity; that is, wind disturbances vary in form of a cosine function with a magnitude of 10 m/s. Simulation results concerning the inaccurate model parameters and wind disturbance are shown in Figs. 7 and 8.

Fig. 7 presents the simulation results of circle trajectory tracking with inaccurate parameters and wind disturbances. The solid line represents the actual trajectory, whereas the dotted line represents the desired time-varying trajectory. From Fig. 7, we conclude that the proposed control scheme can track the desired trajectory accurately despite parameter uncertainties and external disturbances.

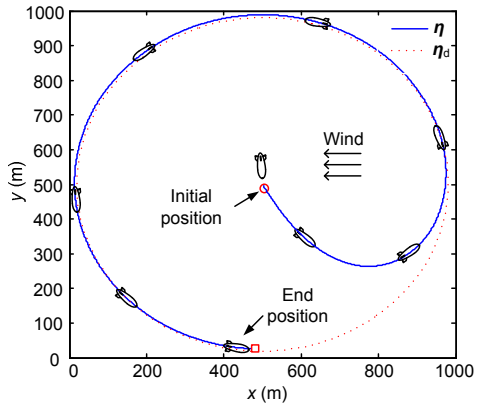

Fig. 7 Circle trajectory tracking with inaccurate parameters and disturbances

The tracking errors in position and orientation are shown in Fig. 8a. In contrast to Case 1, the position error in the x-direction converges to a very small neighborhood of zero, of the order of 3 m.

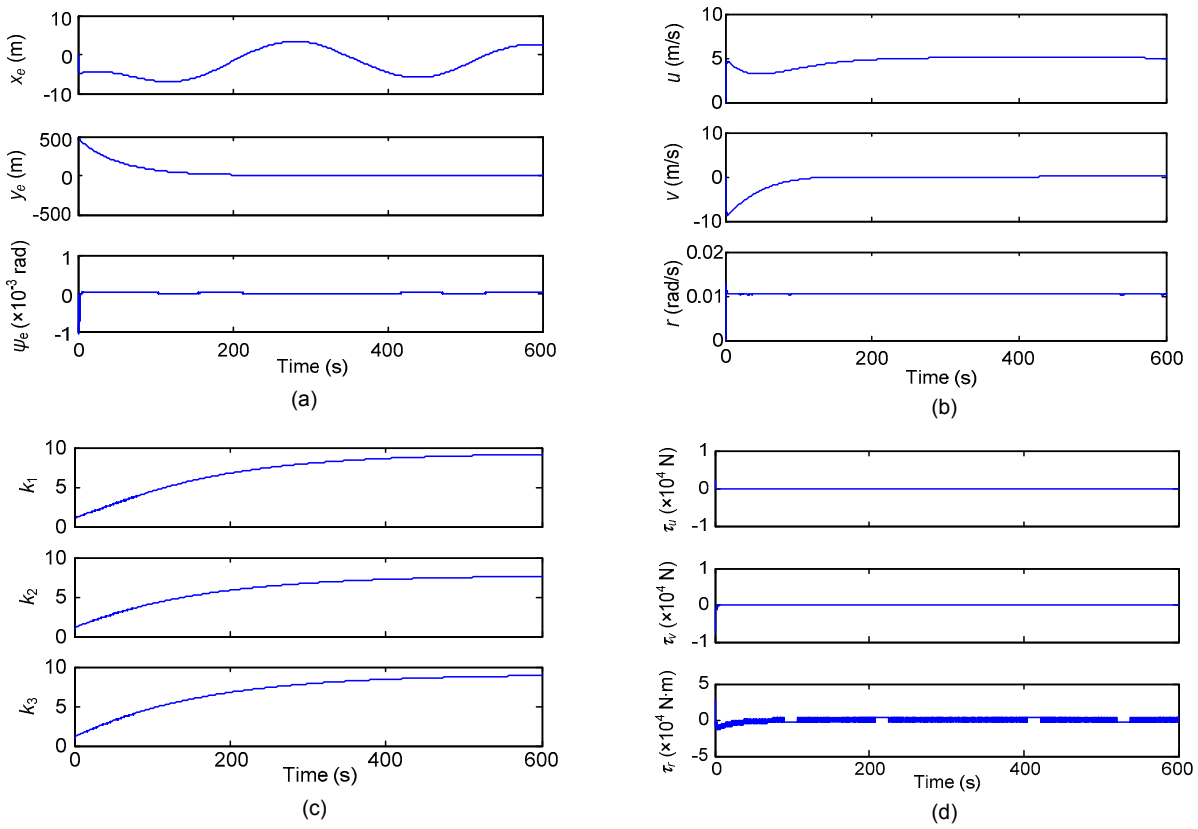

Fig. 8 Tracking errors (a), generalized velocities (b), control gains (c), and control inputs (d) with inaccurate parameters and disturbances

The position error in the y-direction and the orientation error gradually converge to zero. These simulation results demonstrate that the designed control scheme accomplishes trajectory tracking precisely despite parameter uncertainties and external disturbances.

The general velocities are depicted in Fig. 8b. In contrast to Case 1, they converge to a stable value a little later. Despite parameter uncertainties and external disturbances, the actual velocities can also be controlled to track the desired velocities.

The evolution of control gains is depicted in Fig. 8c. The control gain converges to a certain constant value after trajectory tracking is accomplished. The values of the control gains are different from those in Case 1 due to the parameter uncertainties and external disturbances.

As shown by the transition curves of the control inputs in Fig. 8d, the control inputs actualize the trajectory tracking in the presence of parameter uncertainties and external disturbances. In contrast, the control inputs τ_v and τ_r are a little different from those in the case with accurate parameters and without external disturbances.

5 Conclusions

In this paper, an FASMC scheme is proposed for designing a trajectory tracking control system of an autonomous airship. The trajectory control problem is first formulated for an airship. Then, the SMC law is designed to track a time-varying reference trajectory for its robustness and finite time convergence. To achieve a capacity for highly accurate trajectory control, a fuzzy control system is proposed in which the control gains are tuned according to the fuzzy rules, and an adaptation law is used to estimate the model uncertainties. Simulation results demonstrate that the FASMC scheme performs well in terms of stability and robustness of trajectory tracking control despite parameter uncertainties and external disturbances.

Future work will involve the addition of actuator dynamics in the control system of an airship. The dynamic characteristics of the aerodynamic surface, vectored trust, and ballonet should be analyzed, and control allocation among these actuators has to be investigated.

References

Bagheri, A., Moghaddam, J.J., 2009. Simulation and tracking control based on neural-network strategy and sliding-mode control for underwater remotely operated vehicle. *Neurocomputing*, **72**(7-9):1934-1950. [doi:10.1016/j.neucom.2008.06.008]

Cai, Z.L., 2006. Research on Dynamical Modeling and Nonlinear Control of a Stratospheric Airship. PhD Thesis, Shanghai Jiao Tong University, Shanghai, China (in Chinese).

Cai, Z.L., Qu, W.D., Xi, Y.G., 2007. Stabilization of an under-actuated bottom-heavy airship via inter-connection and damping assignment. *Int. J. Robust Nonl. Control*, **17**(18): 1690-1715. [doi:10.1002/rnc.1187]

Chu, A., Blackmore, M., 2007. Novel Concept for Stratospheric Communications and Surveillance: Star Light. AIAA Balloon System Conf., p.1-9.

Dong, C.Y., Xu, L.J., Chen, Y., 2009. Networked flexible spacecraft attitude maneuver based on adaptive fuzzy sliding mode control. *Acta Astronaut.*, **65**(11-12):1561-1570. [doi:10.1016/j.actaastro.2009.04.004]

Fateh, M.M., 2010. Robust fuzzy control of electrical manipulators. *J. Intell. Robot. Syst.*, **60**(3-4):415-434. [doi:10.1007/s10846-010-9430-y]

Filoktimon, R., Evangelos, P., 2008. Robotic Airship Trajectory Tracking Control Using a Backstepping Methodology. IEEE Int. Conf. on Robotics and Automation, p.188-193.

Lee, S.J., Lee, H.C., 2007. Backstepping Approach of Trajectory Tracking Control for the Mid-altitude Unmanned Airship. AIAA Guidance, Navigation and Control Conf. and Exhibition, p.1-14.

Li, J., Zhou, S., Xu, S., 2008. Fuzzy control system design via fuzzy Lyapunov functions. *IEEE Trans. Syst. Man Cybern. B*, **38**(6):1657-1661. [doi:10.1109/TSMCB.2008.928224]

Li, X.R., Zhao, L.Y., Zhao, G.Z., 2005. Sliding mode control for synchronization of chaotic systems with structure or parameters mismatching. *J. Zhejiang Univ. Sci.*, **6A**(6): 571-576. [doi:10.1631/jzus.2005.A0571]

Li, Y.W., Nahon, M., Sharf, I., 2009. Dynamics modeling and simulation of flexible airships. *AIAA J.*, **47**(3):592-605. [doi:10.2514/1.37455]

Liu, H.S., Zhu, S.Q., Chen, Z.W., 2010. Saturated output feedback tracking control for robot manipulators via fuzzy self-tuning. *J. Zhejiang Univ.-Sci. C (Comput. & Electron.)*, **11**(12):956-966. [doi:10.1631/jzus.C0910772]

Liu, J.K., 2008. Control System Design and Matlab Simulation of Robots. Tsinghua University Press, Beijing, China (in Chinese).

Moutinho, A., Azinheira, J.R., 2005. Stability and Robustness Analysis of the AURORA Airship Control System Using Dynamic Inversion. IEEE Int. Conf. on Robotics and Automation, p.2265-2270.

Murguia-Rendon, G., Rodriguez-Cortes, H., Velasco-Villa, M., 2009. Trajectory Tracking Control for the Planar Dynamics of a Thrust Vectored Airship. 52nd IEEE Int. Midwest Symp. on Circuits and System, p.329-332. [doi:10.1109/MWSCAS.2009.5236089]

Neila, M.B., Damak, T., 2011. Adaptive terminal sliding mode control for rigid robotic manipulators. *Int. J. Autom. Comput.*, **8**(2):215-220. [doi:10.1007/s11633-011-0576-2]

Schafer, I., Reimund, K., 2002. Airships as Unmanned Platforms: Challenge and Chance. AIAA's Aircraft Technology, Integration, and Operations, p.1-10.

Sun, F.C., Sun, Z.Q., Feng, G., 1999. An adaptive fuzzy controller based on sliding mode for robot manipulators. *IEEE Trans. Syst. Man Cybern. B*, **29**(4):661-667.

Tong, S.C., Li, H.X., 2003. Fuzzy adaptive sliding-mode control for MIMO nonlinear systems. *IEEE Trans. Fuzzy Syst.*, **11**(3):354-360. [doi:10.1109/TFUZZ.2003.812694]

Yang, J.G., Wang, K., Yang, H.Y., Zhang, J.M., 2000. A real-time adaptive control algorithm using neural nets with perturbation. *J. Zhejiang Univ. Sci.*, **1**(1):61-65. [doi:10.1631/jzus.2000.0061]

Yang, Y.N., Wu, J., Zheng, W., 2011a. Dynamics Modeling and Maneuverability Analysis of a Near-Space Earth Observation Platform. Proc. 5th Int. Conf. on Recent Advances in Space Technologies, p.223-226. [doi:10.1109/RAST.2011.5966828]

Yang, Y.N., Zheng, W., Wu, J., 2011b. Sliding Mode Control for a Near-Space Autonomous Airship. 2nd Int. Conf. on Electric Information and Control Engineering, p.3576-3579. [doi:10.1109/ICEICE.2011.5778198]

Yang, Y.N., Wu, J., Zheng, W., 2011c. Vector modeling and stability analysis of a near-space Earth observation platform. *J. Natl. Univ. Defense Technol.*, **33**(3):28-32 (in Chinese).

Yang, Y.N., Wu, J., Zheng, W., 2012. Design, modeling and control for a stratospheric telecommunication platform. *Acta Astronaut.*, in press. [doi:10.1016/j.actaastro.2012.05.010]

Zhang, Y., 2009. Modeling and Control System Design for Autonomous Airship. PhD Thesis, Shanghai Jiao Tong University, Shanghai, China (in Chinese).

Zhang, Y., Qu, W.D., Xi, Y.G., Cai, Z.L., 2008a. Stabilization and trajectory tracking of autonomous airship's planar motion. *J. Syst. Eng. Electron.*, **19**(5):974-981. [doi:10.1016/S1004-4132(08)60184-X]

Zhang, Y., Qu, W.D., Xi, Y.G., Cai, Z.L., 2008b. Adaptive stabilization and trajectory tracking of airship with neutral buoyancy. *Acta Autom. Sin.*, **34**(11):1437-1440. [doi:10.3724/SP.J.1004.2008.01437]